

Radiation influence model in MWIR hyperspectral simulation

Li Bo, Wang Xiangfeng, Sun Lina, Cui Yan

(Shenyang Institute of Engineering, Shenyang 110136, China)

Abstract: In order to improve the fidelity of the IR hyperspectral target characteristic simulation, an influence model was presented in this paper to calculate the influence of the nearby building on the target final radiation at certain wavelength. A virtual experiment scene was constructed with 1976 U.S. standard atmosphere. Simulation experiments were done based on the constructed virtual scene in 3.0–5.0 μm at intervals of 0.01 μm , and the calculation results were compared with the target reflected solar radiation and the target self-radiation. Experiments results show that the radiation influence from the building are higher than the target reflected solar radiation or the target self-radiation at some waveband ranges, which means the radiation influence is the most critical radiation in some images of the image cube. It proves the influence model presented in this paper is necessary and important in hyperspectral simulation. Through the analysis of simulation results, the building surface temperature, atmosphere transmittance and the valid radiation area are determined to be the 3 key factors to affect the influence radiation of nearby building.

Key words: radiation influence; atmosphere transmittance; reflectance; reflected solar radiation

CLC number: TJ765 **Document code:** A **DOI:** 10.3788/IRLA201847.0304003

中波红外高光谱仿真中的辐射影响模型

李 波,王祥凤,孙丽娜,崔 妍

(沈阳工程学院, 沈阳 辽宁 110136)

摘 要: 为提高红外高光谱目标特性仿真的逼真度,提出了一种辐射影响计算模型,用于计算目标周围的建筑物对目标的最终辐射特性的影响。建立了一个虚拟实验场景,设定场景的大气环境为 1976 年的美国标准大气。在建立的虚拟场景上在中波红外 3.0~5.0 μm 范围内以 0.01 μm 为步长对目标所受的辐射影响进行了仿真计算,并将辐射影响与太阳辐射、目标自身辐射进行了比较。实验结果显示在中波红外的某些波段范围内,相邻建筑单位面积的辐射影响亮度要高于太阳辐射亮度和目标自身辐射亮度。这表明在图像立方体的某些图像中,辐射影响是成像的最主要的辐射源,证明了多光谱/高光谱仿真情况下该模型的必要性和重要性。通过对仿真结果的分析,确定了建筑表面温度、大气透过率和有效辐射面积是辐射影响因素中的三个关键因素。

关键词: 辐射影响; 大气透过率; 反射率; 反射的太阳辐射

收稿日期:2017-10-10; 修订日期:2017-11-20

基金项目:辽宁省自然科学基金(2015020020);辽宁省教育厅科研项目(L2015368,L201602,LQN201709,L15BGL035);沈阳市科技计划项目(18-015-7-29)

作者简介:李波(1980-),男,副教授,博士,主要从事虚拟现实与仿真技术方面的研究。Email:lbian@126.com

通讯作者:王祥凤(1981-),女,高级工程师,主要从事高光谱仿真技术方面的研究。

0 Introduction

With the application and development of infrared imaging technology, the infrared multispectral/hyperspectral imaging technology has become the new generation of photoelectric detection technology^[1-3], and has been widely used in many fields such as military, agriculture, industry, biology and so on. Compared with traditional IR images, the hyperspectral images can provide more information in form of image cube, which merges the spatial information and spectral information. In the development of relevant instruments, equipments and the validation of relevant algorithm^[4], plenty of hyperspectral images are needed. The images acquired from relevant equipments are expensive, and it is impossible to capture images in various meteorological environment on the other hand. As a result, the infrared hyperspectral simulation technology has become a new research hotspot.

The infrared hyperspectral simulation technology is developed from traditional infrared simulation technology^[5]. The images from traditional infrared simulation technology focus on the overall radiation status of a wide waveband range like 3–5 μm and 8–12 μm , which ignore the radiation characteristic of every single tiny waveband range like 3.04–3.05 μm and 9.25–9.26 μm , while the hyperspectral images can exactly show the radiation differences between tiny waveband ranges. The radiation differences have important significance in many fields such as target detection and identification, IR-counter-countermeasures^[6] and so on. At the meantime, the hyperspectral simulation requires much more precise data, because any tiny data noise may influence the effect of the simulation images. Therefore, as many as possible factors should be involved in the hyperspectral simulation^[7]. And the hyperspectral

simulation should not use the way of traditional IR simulation directly because of the ignorance of tiny waveband rang characteristic.

A radiation influence model for the hyperspectral target radiation characteristic simulation is proposed in this paper. The model is used to calculate the radiation influence on the target radiation from a nearby building in the waveband rang of 3–5 μm at intervals of 0.01 μm based on a virtual scene. The calculation results show the radiation differences among tiny wavebands and the importance and necessity of the radiation influence model.

The research work in this paper shows that some factors which needn't to be considered in the wide waveband simulation (like 3.0–5.0 μm) could be very important which can decide whether the simulation result is correct in some tiny waveband. The result has very important guiding meaning to the determination of necessary factors in the IR hyperspectral simulation.

1 Establishment of the model

The main factors for the target radiation characteristic simulation in the traditional IR simulation are the target self-radiation and the reflected radiation of the target from environment, while the environment radiation including the solar radiation, the atmosphere radiation and the ground radiation is shown in formula(1):

$$L_{\text{obj}}(\lambda) = L_{\text{objself}}(\lambda) + L_{\text{rsun}}(\lambda) + L_{\text{rground}}(\lambda) + L_{\text{rsky}}(\lambda) \quad (1)$$

The formula (1) is not precise enough to simulate the target characteristic in the hyperspectral simulation because of the ignorance of the radiation influence. For example, if the target is beyond a building, the building will influence the radiation characteristic of the target. The influence effect is especially obvious in hyperspectral simulation, and can't be shown by formula (1).

A virtual scene is constructed as shown in Fig.1. There is a target in the scene, whose surface is

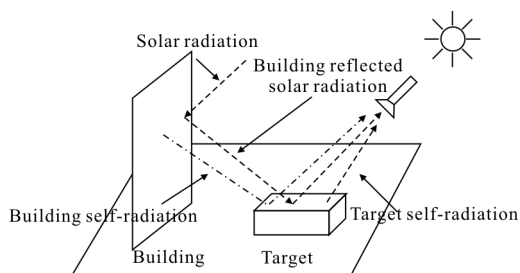


Fig.1 Virtual scene

made of aluminium alloy. A concrete building is located 100 m far from the target, whose outer wall is rough enough to work as a Lambert reflecting plane. Setting the atmosphere of the virtual scene is 1976 US standard atmosphere, the weather is clean and calm, the visibility on the ground is 23 km, the aerosol model of near ground is typical aerosol model. The cloud effect and convection is unconsidered in the virtual scene. The sun is in the 200th day in a year, the zenith angle and azimuth angle are 30°. All the reflection by the target and the building in the scene is set as Lambertian reflection.

In view of this situation, the influence calculation model is proposed to achieve more precise simulation of the target characteristic.

$$L_{obj}(\lambda) = L_{objself}(\lambda) + L_{rsun}(\lambda) + L_{rground}(\lambda) + L_{rsky}(\lambda) + L_{infl}(\lambda) \quad (2)$$

Where $L_{infl}(\lambda)$ is the calculation item of the radiation influence for the target from nearby buildings.

Considering the fact that the solar radiation and the target self-radiation are two most important items in the process of IR detection, if some radiation could be compared to this two radiation, then the radiation should not be ignored. In order to describe the importance of the radiation from nearby buildings, the research of the zero stadia radiation characteristic of the target is mainly focused on these two factors, and

the ground radiation the atmosphere radiation are ignored in this paper.

As shown in Fig.1, the radiation influence of the target which can be calculated by formula(3) is mainly from the self-radiation of the nearby building and the reflected solar radiation of the nearby building.

$$L_{infl}(\lambda) = L_{rb}(\lambda) + L_{rbsun}(\lambda) \quad (3)$$

Where $L_{rb}(\lambda)$ is the target reflected radiation from nearby building, and $L_{rbsun}(\lambda)$ is the target reflected radiation from the nearby building reflected solar radiation.

In the process of radiation transmission, the atmosphere will result in an absorption loss to the radiation. The reflected radiation of a point on the target from per unit area of the nearby building can be calculated as in formula (4), which is related to the atmosphere transmittance and the reflectivity of the material of the outer wall of the building.

$$L_{rbu}(\lambda) = L_{bp}(\lambda, T) \times \xi(\lambda) \times \rho_t(\lambda) \quad (4)$$

Where $L_{bp}(\lambda, T)$ is the radiance of waveband λ at temperature T of a unit valid radiation area, $\xi(\lambda)$ is the atmosphere transmittance at waveband λ , and $\rho_t(\lambda)$ is the reflectance of the target surface at waveband λ .

For any point P on the target surface, the total radiation from the nearby building is related to the valid radiation area for point P , as shown in Fig.2. The total radiation P received could be described in formula (5):

$$L_{rb}(\lambda) = \int_0^S L_{rbu}(\lambda) ds = \int_0^S L_{bp}(\lambda, T) \times \xi(\lambda) \times \rho_t(\lambda) ds \quad (5)$$

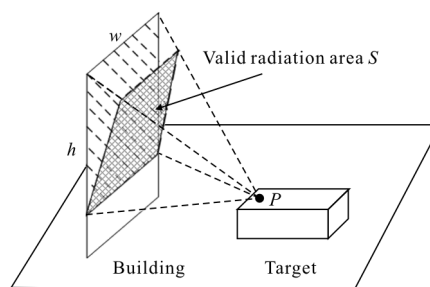


Fig.2 Valid radiation area to P

Where S is the valid radiation area to point P .

Assuming the outer wall of the nearby building is lambert body because of its roughness, which means the solar radiation reflected by the outer wall has the same intensity at all direction. The building reflected solar radiation will be reflected by the target surface, after the absorption of the atmosphere, and finally achieve the sensor. The radiation from a unit valid radiation area received by point P on the target surface could be described as formula (6):

$$L_{rbsun}(\lambda) = L_{sun}(\lambda) \times \rho_b(\lambda) \times \xi(\lambda) \times \rho_t(\lambda) \quad (6)$$

Where $L_{sun}(\lambda)$ is the solar radiance, and $\rho_b(\lambda)$ is the material reflectance of the building outer wall at waveband λ .

The radiation amount received by point P is related to the valid radiation area of the nearby building to P . The radiance P received from the nearby building reflected solar radiation could be described as formula (7):

$$L_{rbsun}(\lambda) = \int_0^S L_{sun}(\lambda) \times \rho_b(\lambda) \times \xi(\lambda) \times \rho_t(\lambda) ds \quad (7)$$

The final radiation influence calculation formula of point P could be derived by formula (3)–(7) as formula (8):

$$L_{infl}(\lambda) = \int_0^S (L_{bp}(\lambda, T) + L_{sun}(\lambda) \times \rho_b(\lambda)) ds \times \xi(\lambda) \times \rho_t(\lambda) \quad (8)$$

2 Simulation calculation

For simulation, the atmosphere of the virtual scene is set as U.S. standard atmosphere in 1976, date is early in July, sunny with 30° solar zenith angle, ignoring the absorption effect from aerosols or clouds. Assuming the material of the target surface is aluminium, the material of building outer wall is construction concrete. The surface temperature of both the target and the building is 300 K. The simulation calculation is done in waveband $3.0\text{--}5.0 \mu\text{m}$.

2.1 Self-radiation of the target

The self-radiation of target at wavelength λ is

related to the surface temperature T and the emittance $\varepsilon(\lambda)$ of the surface material at wavelength λ . According to Planck law of black-body radiation, the radiation exitance of black-body of temperature T at wavelength λ is:

$$M_{black}(\lambda, T) = \frac{2\pi hc^2}{\lambda^5 \left(e^{\frac{hc}{\lambda kT}} - 1 \right)} c_1 / \left[\lambda^5 \left(e^{\frac{c_2}{\lambda T}} - 1 \right) \right] \quad (9)$$

Where h is the Planck constant, k is the Boltzmann constant, c is the speed of light, and T is the thermodynamic temperature. $c_1 = 2\pi hc^2 = 3.7418 \times 10^{-16} (\text{W} \cdot \text{m}^2)$ and $c_2 = \frac{hc}{k} = 1.4388 \times 10^4 (\mu\text{m} \cdot \text{K})$ are called the first and second radiation constant.

The radiation exitance of common body whose emittance at wavelength λ is $\varepsilon(\lambda)$ could be calculated as in formula (10):

$$M(\lambda, T) = \varepsilon(\lambda) \times M_{black}(\lambda, T) \quad (10)$$

The radiance of the common body is:

$$L(\lambda, T) = \varepsilon(\lambda) \times M_{black}(\lambda, T) / \pi \quad (11)$$

Supposing the transmittance of concrete outer wall and the target surface are both 0, then the emittance of the material could be calculated by the material reflectance which could be acquired from the U.S. JPL (Jet Propulsion Laboratory) ASTER Spectral Library^[8] as in formula (12):

$$\varepsilon(\lambda) = 1 - \rho(\lambda) \quad (12)$$

The reflectance of aluminium in waveband $3.0\text{--}5.0 \mu\text{m}$ from ASTER Spectral Library is shown in Fig.3, and the corresponding emittance is shown in Fig.4.

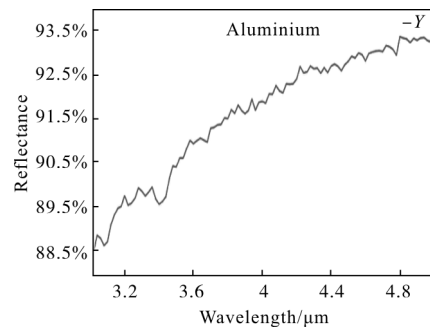


Fig.3 Reflectance of aluminium in $3.0\text{--}5.0 \mu\text{m}$

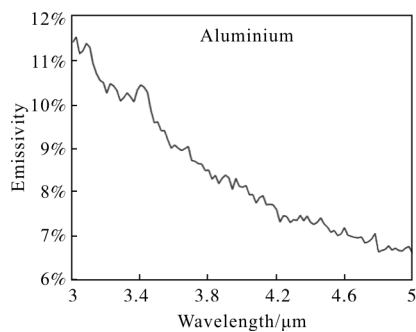


Fig.4 Emittance of aluminium in 3.0-5.0 μm

According to formula (11), the calculation result of self-radiance of the target at 300 K is shown in Fig.5.

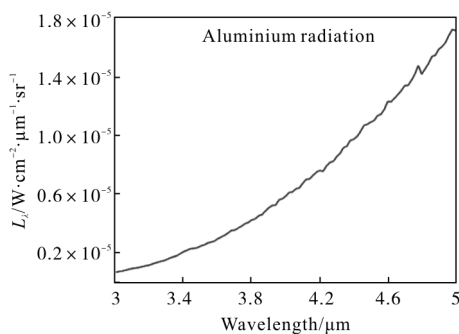


Fig.5 Radiance of aluminium in 3.0-5.0 μm

2.2 Target reflected solar radiation

In this paper, the sun is considered to be a constant light source. The solar radiation has very important influence in the process of IR hyperspectral simulation. Below is the computation formula of target reflected solar radiance $L_{rsun}(\lambda)$:

$$L_{rsun}(\lambda) = L_{sun}(\lambda) \times \rho_t(\lambda) = I_{sun}(\lambda) \times \rho_t(\lambda) / \pi \quad (13)$$

Where $I_{sun}(\lambda)$ is the solar direct irradiance which could be calculated by Modtran, $\rho_t(\lambda)$ is the reflectance of the target surface material at wavelength λ .

The result of the solar irradiance for the scene calculated by Modtran in waveband 3.0-5.0 μm is shown in Fig.6.

According to formula (13), the calculated result of target reflected solar irradiance is shown in Fig.7.

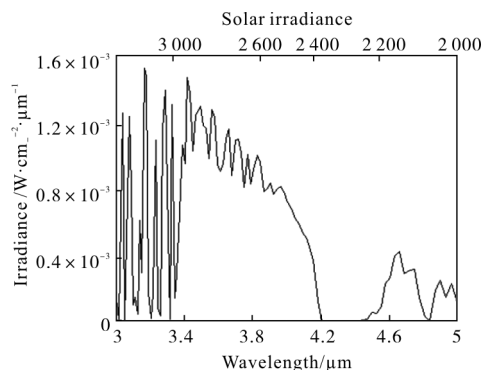


Fig.6 Solar irradiance

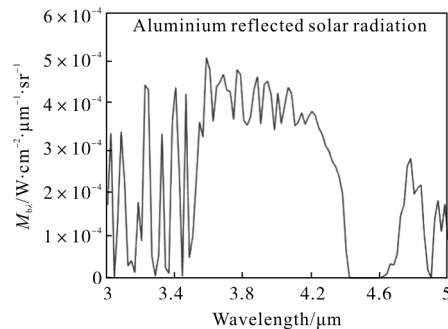


Fig.7 Target reflected solar radiance

2.3 Target reflected self-radiation of building

The reflectance of construction concrete acquired from JPL ASTER Spectral Library is shown in Fig.8, and the emittance is shown in Fig.9.

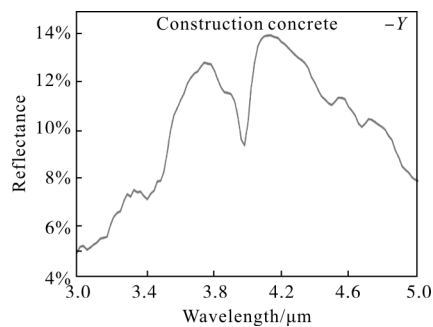


Fig.8 Reflectance of construction concrete

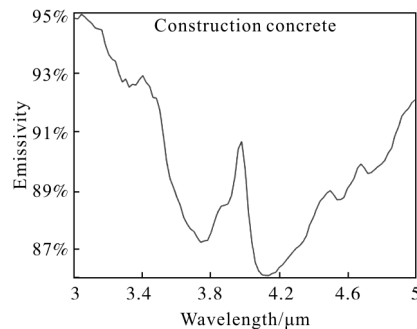


Fig.9 Emittance of construction concrete

The temperature of the nearby building outer wall is 300 K. According to formula (11), the calculation result of the self-radiance of the outer wall is shown in Fig.10.

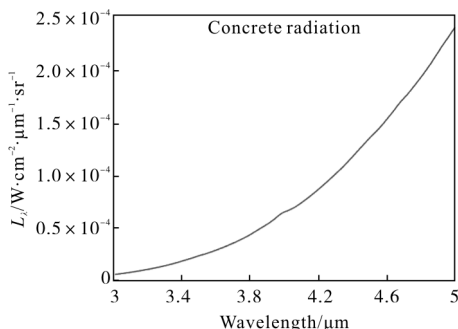


Fig.10 Self-radiance of the nearby building

In current atmosphere, the IR radiation atmosphere transmittance in distance of 100 m in waveband range 3.0–5.0 μm calculated by Modtran is shown in Fig.11. According to the calculation results, the transmittance is extremely high in almost all the waveband range except for 4.2–4.3 μm, where the transmittance deduced to 0 rapidly. Figure 11 shows clear evidence that the radiance from the building can reach the target with only a tiny energy loss.

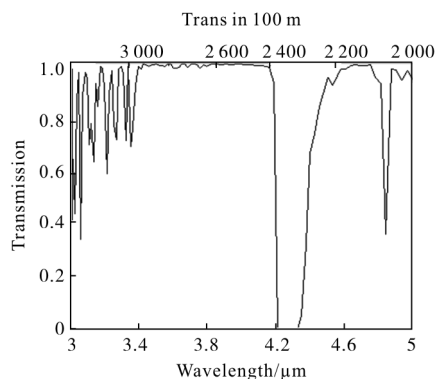


Fig.11 Transmittance in 100 m

The calculation results of radiance reaches the target from one unit of the nearby building is shown in Fig.12.

According to formula (4), the target reflected radiance from one unit of the nearby building is shown in Fig.13.

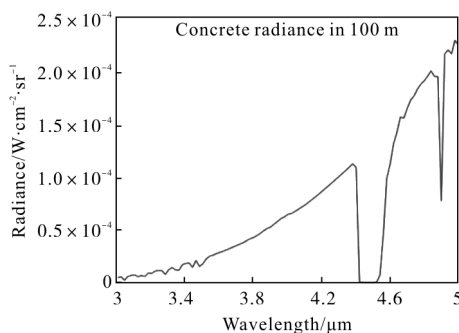


Fig.12 Radiance from one unit of the nearby building

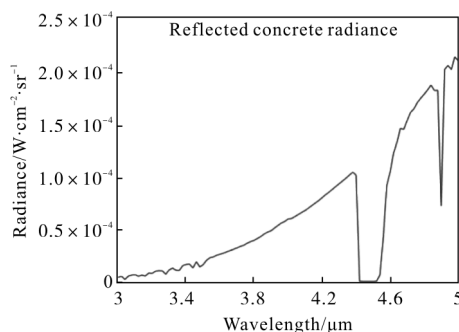


Fig.13 Target reflected radiance from one unit of the nearby building

2.4 Target reflected radiance from the nearby building reflected solar radiance

According to formula (6), considering the building as a Lambert body, the calculated results of target reflected radiance from one unit of the nearby building reflected solar radiance is shown in Fig.14.

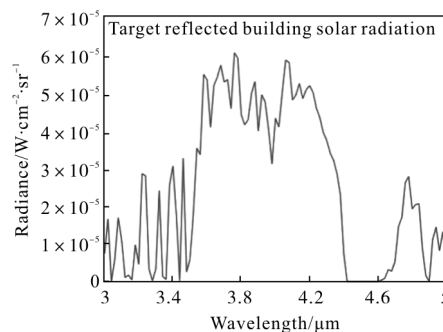


Fig.14 Target reflected radiance from the nearby building reflected solar radiance

2.5 Radiation influence from one unit of the nearby building

According to formula (8), the radiation influence from the nearby building is related to the building self-radiance and the building

reflected solar radiation. The total radiation influence to point P from one unit for nearby building is shown in Fig.15.

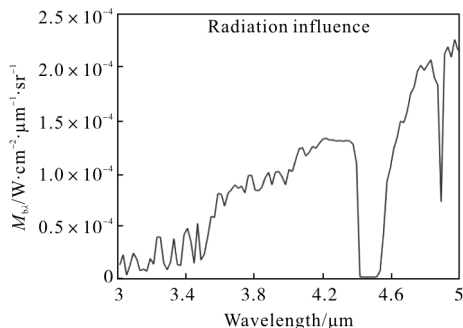


Fig.15 Total radiation influence

So far, all the 4 critical factors in the scene which can influence the target final radiation characteristics are calculated. Put the 4 calculation results together for comparison in one single figure as shown in Fig.16. The reflected building self-radiation and the reflected solar radiation from building are the radiation influence to the target. Figure 16 shows clear evidence that the solar radiation is the most critical factor in the scene in waveband range 3.0–5.0 μm , while the target self-radiation is at a pretty low level. The building reflected solar radiation is higher than the building self-radiation in wavelength band 3.0–3.9 μm , while the building self-radiation is much higher than the building reflected solar radiation in wavelength band 3.9–5.0 μm .

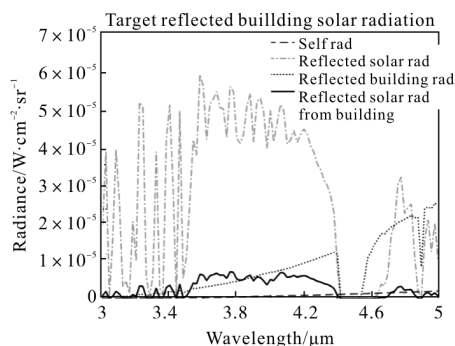


Fig.16 4 critical radiation factors

3 Analysis of the simulation results

Put the target self-radiation, the target

reflected solar radiation and the building radiation influence to the target which is combined with the reflected building self-radiation and the reflected solar radiation from the building together in one single figure as shown in Fig.17.

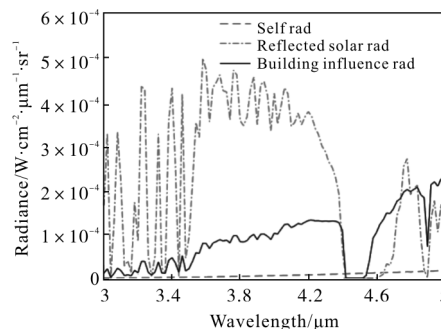


Fig.17 Radiation comparison in the scene

Figure 17 shows that the solar radiation is dozens of times to hundreds to the target self-radiation in entire waveband range 3.0–5.0 μm . That's why the target self-radiation could be ignored in traditional IR simulation in waveband 3.0–5.0 μm . But for hyperspectral IR simulation which focuses on the differences in one single wavelength, the target self-radiation should not be ignored. For example, in wavelength 4.9 μm , the target self-radiation is higher than the solar radiation.

According to the calculation results, the radiation influence from the building and the solar radiation in the virtual scene are at the same order of magnitude. In the waveband range 3.0–4.4 μm , the radiation influence is several times smaller than the solar radiation, while it is bigger in 4.4–5.0 μm . The calculation results prove that the radiation influence is more important than the solar radiation in some wavelength range, and should be seriously considered in the simulation process.

3.1 Influence with changes of the valid radiation area

The calculation results shown in Fig.17 are based on the radiation from one single unit from

the nearby building. With the increase of the valid radiation area, the influence effect becomes larger and larger, and the radiation from the building becomes the most important radiation in more and more wavelengths. As shown in Fig.18, when doubling the valid radiation area, the radiation from the building becomes the most important radiation in 4.3–5.0 μm . When tripling the valid radiation area, the radiation influence becomes the most important radiation in 4.2–5.0 μm . When quadrupling the valid radiation area, the radiation influence becomes the most important radiation in 4.0–5.0 μm . At the meantime, the radiation influences in other waveband are enhanced obviously. According to the calculation, when the valid radiation area increased by 12 times, the radiation influence will become the most important radiation in 3.0–5.0 μm .

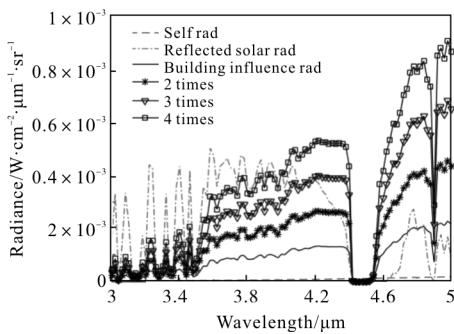


Fig.18 Radiation influence with different valid radiation area

3.2 Influence with changes of the surface temperature of the nearby building

Figure 19 shows the comparison of the target reflected self-radiation of the building at different temperatures with the target self-radiation and the target reflected solar radiation at one single unit radiation area. The figure reveals that the self-radiation of the building is not higher than the building reflected solar radiation in 3.0–4.2 μm , while the self-radiation is much higher than the building reflected radiation in waveband 4.2–5.0 μm when the building's temperature is less than 290 K.

When the temperature is higher than 290 K, the self-radiation of the building is stronger than the solar radiation in 3.0–5.0 μm . As the temperature increases, the influence level improves significantly.

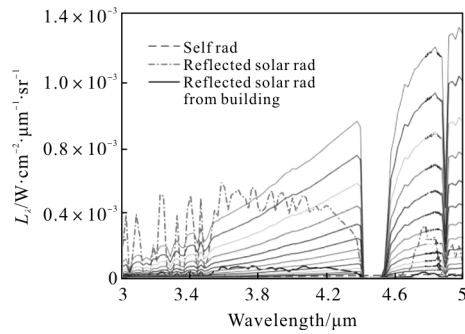


Fig.19 Comparison of the radiation at different temperatures

The study shows that surface temperature of the building has an obvious effect on the radiation characteristic of target, and the influence effect become stronger in hyperspectral simulation conditions especially.

4 Conclusion

Aiming at the characteristic of the IR hyperspectral simulation and buildings that are made of concrete, the radiation influence model is presented in this paper for the target IR characteristic simulation with a nearby building. And simulation experiments are done in a constructed virtual scene in waveband range 3.0–5.0 μm .

The simulation experiments results show that the radiation from the nearby building has huge influence on the final radiation characteristic of the target. The surface temperature of the nearby building, the valid radiation area and the distance from the target to the building are critical factors for the target final radiation characteristic.

To sum up in conclusion, in IR hyperspectral simulation, the nearby buildings of the target can cause huge influence on the target final radiation characteristic at some wavelength. Therefore the nearby building factor should be serially

considered in hyperspectral simulation. The radiation influence model presented in this paper could calculate the radiation influence effectively and precisely.

References :

- [1] Xu Hong, Wang Xiangju n. Applications of multispectral/hyperspectral imaging technologies in military [J]. *Infrared and Laser Engineering*, 2007, 36(1): 13–19. (in Chinese)
- [2] Zheng Weijian, Lei Zhenggang, Yu Chunchaoe, et al. Research on ground-based LWIR hyperspectral imaging remote gas detection[J]. *Spectroscopy and Spectral Analysis*, 2016, 36(2): 599–606. (in Chinese)
- [3] Xie Feng, Liu Chengyu, Shao Honglan, et al. Scene-based spectral calibration for thermal infrared hyperspectral data[J]. *Infrared and Laser Engineering*, 2017, 46(1): 0138001. (in Chinese)
- [4] Cheng Mengshuo, Qian Yongqiang, Wang Ning, et al. A temperature and emissivity retrieval algorithm based on atmospheric absorption feature from hyperspectral thermal infrared data [J]. *J Infrared Millim Waves*, 2016, 35(10): 617–624. (in Chinese)
- [5] Li Bo, Zhao Huaici, Hua Haiyang. Radiation influence research between buildings in IR multispectral simulation[J]. *Infrared and Laser Engineering*, 2014, 43(10): 3222–3227. (in Chinese)
- [6] Wang Yachao, Zhao Huijie, Jia Guorui. Modeling and simulation of topographic effects for hyperspectral remote sensing [J]. *Journal of Beijing University of Aeronautics and Astronautics*, 2010, 36(9): 1131–1134. (in Chinese)
- [7] Yan Peipei, Ma Caiwen, Zhe Wenji. Influence of earth's reflective radiation on space target for space based imaging [J]. *Acta Phys Sin*, 2015, 64(16): 463–470. (in Chinese)
- [8] Baldrige A M, Hook S J, Grove C I, et al. The ASTER spectral library version 2.0 [J]. *Remote Sensing of Environment*, 2009, 113: 711–715.